A Study of Ethylamine at a Gold Rotating Ring-Disk Electrode Using Pulsed Electrochemical Detection at the Ring

David A. Dobberpuhl[+] and *Dennis C. Johnson**[++]

[+]Department of Chemistry, Creighton University, Omaha, NE 68178, USA
[++]Department of Chemistry, Iowa State University, Ames, IA 50011, USA

Received: October 21, 1995
Final version: December 20, 1995

Abstract
Linear scan (cyclic) voltammetry at the disk with simultaneous pulsed electrochemical detection (PED) at the ring of a rotated ring-disk electrode (RRDE) is demonstrated to be applicable for studies of the complex anodic behavior of ethylamine at gold electrodes in 0.10 M NaOH. The oxidation of ethylamine at the disk occurs during positive scans concomitantly with formation of surface oxide (Au → AuOH → AuO). However, the final oxide-covered surface (AuO) is inert for further ethylamine oxidation. Data obtained at the RRDE demonstrate that the total ethylamine signal at the disk is composed of simultaneous contributions from: oxidative desorption of ethylamine preadsorbed at the oxide-free Au surface and oxidation of ethylamine transported to the disk simultaneously with oxide formation. Based on ring-disk data, preadsorbed ethylamine is estimated to correspond to a fractional surface coverage of 0.7 ± 0.1 monolayer for 10 to 60 μM ethylamine. Of this coverage, ca. 75% corresponds to ethylamine coadsorbed reversibly with OH^- and 25% to ethylamine adsorbed irreversibly by a mechanism concluded to be chemisorption.

Keywords: Ethylamine, Gold, Voltammetry, Adsorption

In honor of the retirement of Professor Petr Zuman from Clarkson University

1. Introduction

Because of their biological and industrial importance, the electrochemistry of organic amines has been studied at a variety of metal electrodes, including Cu [1–3], Pt [4–6], Au [7–9], Ag [10–13] and the oxides of Co, Cu, and Ni [13–16]. Primary goals in these studies have included the identification of oxidation product(s) and elucidation of reaction mechanisms. Our laboratory maintains a strong interest in the anodic response of aliphatic amines at noble metal electrodes, including Au, as the basis for pulsed electrochemical detection (PED) of these compounds following their separations by liquid chromatography [17]. A previous study of ethanolamine at Au in alkaline media found that the anodic current is virtually mass-transport limited (i.e., fast heterogeneous kinetics) during the positive potential scan at the oxide-free electrode surface [18]. This result is surprising because the ethanolamine signal comes from oxidation of the alcohol moiety and, yet, almost no signal is obtained for oxidation of ethanol under the same conditions. The large ethanolamine current was attributed to the beneficial effect of adsorption by the amine moiety, which increases the residence time of ethanolamine molecules at the Au surface and enhances the probability for successful oxidation.

A more general study of amine adsorption at Au electrodes followed using results obtained at a Au–Au rotated ring-disk electrode (RRDE) [19]. Because the current for amines quickly decays to negligible values at Au electrodes when using a constant potential, PED was applied to the ring electrode to maintain reactivity for amine detection. The adsorption of aliphatic amines, alkanolamines, and an amino acid, glycine, was described as a function of applied potential. The similarity of amine and alkanolamine behavior was evidence that both classes of compounds adsorb *via* their amine groups. This finding supported previous speculation regarding the role of adsorption in the oxidation mechanism of alkanolamines.

Here, the electrochemistry of ethylamine is further investigated using the RRDE with cyclic voltammetry at the disk and PED at the ring. Specifically, the ring of a Au–Au RRDE is used to determine the role adsorption plays in the oxidation of ethylamine at Au electrodes in 0.1 M NaOH.

2. Experimental

2.1. Reagents

Chemicals were used as received. Ethylamine (Kodak, Aldrich) was a practical grade of 70% (w./w.) in water. Sodium hydroxide used as the supporting electrolyte was prepared either from reagent grade pellets (Fisher Scientific) or a commercially available 50% (w./w.) NaOH solution (Fisher Scientific). Water was purified by passage through two D-45 deionizing tanks (Culligan) followed by a Milli-Q purification system (Millipore). All solutions used in voltammetric experiments were deaerated with N_2.

2.2. Voltammetric Apparatus

Data were obtained using an AFMT28AUAU gold ring-disk electrode, an AFMSR rotator, and an AFRDE4 bipotentiostat (Pine Instrument Co.). The RRDE had a disk radius of 0.228 cm. The inner and outer radii of the ring were 0.246 cm and 0.269 cm, respectively. A saturated calomel electrode (SCE; Fisher Scientific) provided the reference potential and a coiled Pt wire was the counter electrode. The electrochemical cell was constructed from Pyrex with porous glass frits separating the working, reference, and counter electrode compartments. The potentiostat was interfaced to a personal computer (PC, Jameco) using a DT2801-A data acquisition board (Data Translation) and ASYST 4.0 software (Keithley/Asyst).

  1040-0397/96/0808-726 $ 10.00+.25/0

2.3. Voltammetry Procedures

Ring-disk procedures have been described [19] and only a brief summary is given here. The disk potential (E_d) was scanned according to a cyclic waveform generated by analog circuitry within the bipotentiostat. The ring potential was controlled according to a multi-step waveform shown in Figure 1. This waveform was generated using a PC and ASYST software. The total time of the PED waveform determined the current sampling frequency, which typically was 2 Hz.

3. Results and Discussion

3.1. Residual Response of Gold Electrodes

Figure 2 shows a typical residual voltammetric (*i-E*) response for the Au disk electrode in deaerated 0.10 M NaOH. The most significant features observed during the positive scan are: charging of the electrical double layer from −1.0 to −0.5 V; adsorption of OH^- from −0.5 to 0.1 V; formation of inert surface oxide (AuO) from 0.15 to 0.7 V; and onset of O_2 evolution at *ca.* 0.6 V. Significant features observed during the subsequent negative scan from 0.7 V are: a rapid attenuation of current caused by the abrupt cessation of O_2 evolution and oxide formation in the region 0.7 to 0.6 V; a large cathodic peak corresponding to reduction of surface oxide from 0.3 to −0.1 V; desorption of adsorbed OH^- from −0.1 to −0.5 V; and double-layer charging from −0.5 to −1.0 V.

The potential regions *ca.* −0.5 V to 0.1 V (positive scan) and −0.1 to −0.5 V (negative scan) have special significance in this study and deserve additional comment. Whereas the processes in these regions are designated as corresponding to adsorption and desorption of OH^-, the exact nature of the adsorbed species is still under speculation. Because the potential −0.5 V corresponds to the potential of zero charge (PZC) in the double layer, some authors conclude the process occurring at $E_d > -0.5$ V corresponds to the electrostatic adsorption of OH^- and other anions present as a component of the supporting electrolyte [21–26]. Other authors conclude this process corresponds to electrosorption with charge transfer to produce a fractional monolayer of adsorbed hydroxyl radicals. The possibility of coadsorption of H_2O has been suggested for neutral and acidic solutions [27–29]. Whatever the exact identity of the adsorbed species, its apparent importance for electrocatalysis of numerous oxidation reactions at gold electrodes has been documented [30–34].

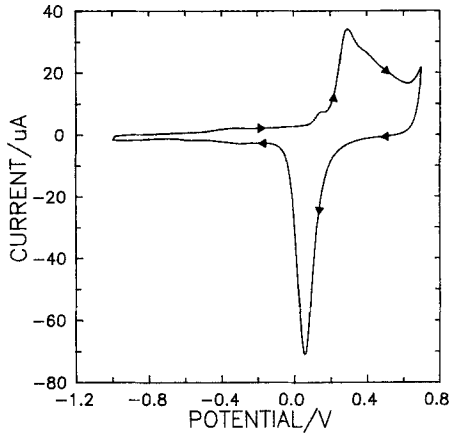

Fig. 2. Residual voltammetric current at the Au RDE in 0.10 M NaOH. Rotational velocity: 94.2 rad s^{-1}. Scan rate: 100 mV s^{-1}.

Also important to this study is the conclusion that formation of surface oxide at $E > +0.15$ V occurs with generation of an intermediate product believed to correspond to an adsorbed hydroxyl radical ($Au + OH^- \rightarrow AuOH + e^-$). The AuOH species has a brief lifetime and ultimately is converted to the inert surface oxide ($AuOH \rightarrow AuO + H^+ + e^-$). The AuOH species has been suggested to be the source of oxygen transported to oxidation products in anodic surface-catalyzed oxygen-transfer reactions.

3.2. Voltammetry of Ethylamine at Gold Electrodes

Voltammetry at the disk electrode of the RRDE was performed to determine contributions to the total disk current (i_d) from oxidative desorption of preadsorbed ethylamine ($i_{d,ads}$) and oxidation of ethylamine arriving at the disk under mass transport control simultaneously with oxide formation ($i_{d,trans}$). Figure 3 contains representative i_d-E_d curves obtained as a function of ethylamine concentration (curves **b**–**e**) in

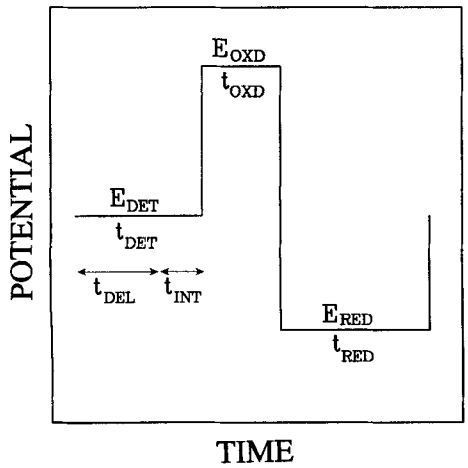

Fig. 1. Potential vs. time for a PED waveform. Definitions: E_{DET}: detection potential (t_{DEL}: delay time, t_{INT}: current integration or averaging time; t_{DET}: $t_{DEL} + t_{INT}$); E_{OXD}: oxidation potential (t_{OXD}: oxidation time); E_{RED}: reduction potential (t_{RED}: reduction time).

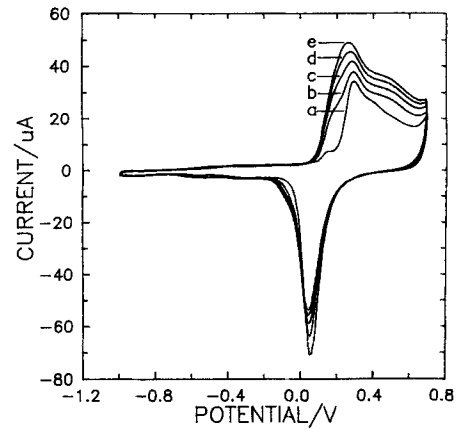

Fig. 3. Voltammetric results for ethylamine at the Au RDE as a function of concentration. Rotational velocity: 94.2 rad s^{-1}. Scan rate: 100 mV s^{-1} Ethylamine concentration [μM]: a) 0; b) 20; c) 40; d) 60; e) 80.

comparison to the residual response (curve **a**). The largest current for the ethylamine is observed during the positive scan from 0.0 V to 0.7 V. Because this anodic current occurs concomitantly with formation of surface oxide, we conclude that the oxidative mechanism is electrocatalytic in nature and is coupled to the oxide-formation process. Nevertheless, the final oxide (AuO) is inert and scan reversal at 0.7 V results in rapid attenuation of the signal for ethylamine oxidation concomitantly with cessation of the current for oxide formation. Hence, attempts to detect aliphatic amines using constant applied potential are unsuccessful.

The rotating disk electrode (RDE) can be used to diagnose if a reaction is transport-limited. According to the Levich equation, transport control is indicated by a linear correspondence between disk current and either the square root of rotational velocity of the electrode ($\omega^{1/2}$, [rad$^{1/2}$ s$^{-1/2}$]) or bulk concentration of reactant (C^b, [mol^3]), as indicated in Equation 1 [20]:

$$i_{d,lim} = 0.62nFAD^{2/3}\omega^{1/2}v^{-1/6}c^b \quad (1)$$

where n is the number of electrons transferred in the reaction ([eq mol^{-1})], F is the Faraday constant [C eq^{-1}], A is the area of the disk electrode [cm^2], and v is the kinematic viscosity of the solution [cm^2 s^{-1}]. A plot (not shown) of the disk current at 0.2 V vs. ethylamine concentration (C^b) with the residual current subtracted exhibits a nearly linear correspondence for small concentrations (< 100 μM), but with a substantial non-zero intercept. Linearity of this i_d–C^b plot satisfies one diagnostic criterion for a transport-limited reaction of ethylamine. However, the nonzero intercept indicates greater complexity in the reaction mechanism, e.g., contribution from the oxidation of ethylamine that is preadsorbed at the oxide-free surface when $E_d < -0.1$ V. A plot of the disk current at ca. 0.2 V vs. C^b deviated from linearity at large ethylamine concentrations (> 100 μM).

Figure 4 contains representative i_d–E_d curves for 40 μM ethylamine as a function of the rotational velocity of the electrode. Plots (not shown) of the maximum values of i_d vs. $\omega^{1/2}$ are nearly linear for low rotational velocities (< 100 rad s^{-1}), but with a substantial nonzero intercept. This is consistent with speculation above that the total anodic current at 0.2 V is the result of oxidation of ethylamine being transported to the electrode as well as ethylamine that has been preadsorbed at the oxide-free surface. Severe deviation from linearity in the $i_d - \omega^{-1/2}$ plot for large rotational velocities (> 100 rad s^{-1}) indicates a finite heterogeneous rate constant for the oxidation reaction.

3.3. Ring-Disk Results for Ethylamine

Rotated ring-disk electrodes (RRDE) are well-suited for investigation of complex reactions involving reactions under control of both surface and transport phenomena. However, applications of the RRDE to studies of organic amines is complicated by the fact that an anodic response cannot be obtained at the ring electrode under conditions of constant applied potential. By applying the multi-step PED waveform shown in Figure 1, the ring of the RRDE can be used successfully to monitor the reaction of amines at the disk [19].

Figure 5 contains typical data obtained at the RRDE in 0.10 M NaOH containing 40 μM ethylamine. Curves **a** and **b** correspond to i_d–E_d curves already discussed for the disk electrode. Curve **c** corresponds to the PED current at the ring electrode as a function of disk potential (i_r–E_d); for clarity, the ring current in Figure 5 is shown multiplied 10× its actual value. The PED detection potential of 0.20 V resulted in the largest signal-to-background ratio for ethylamine, and so was used in this study. The dashed line in Figure 5 represents the steady-state ring current measured with the disk electrode under open-circuit conditions. To aid in this discussion, unique features in the i_r–E_d results (Fig. 5, curve **c**) are given a numerical designation. Region 1 in curve **c** corresponds to the positive scan of E_d and is readily explained based upon the apparent disk response. Here, ring current is diminished from its steady-state value because ethylamine being transported to the RRDE is consumed by the disk reaction. The maximum decrease in the ring current occurs at E_d = ca. 0.2 V. As the disk potential is scanned positive of 0.2 V, the ring current begins to approach its steady state value. However, the disk current from ethylamine in the region ca. 0.4 V $\leq E_d \leq$ 0.7 V remains relatively constant, as indicated by the difference between curves **a** and **b**. Therefore, it is clear that for $E_d \geq 0.4$ V, the majority of the disk current for ethylamine originates from oxidative desorption of preadsorbed ethylamine.

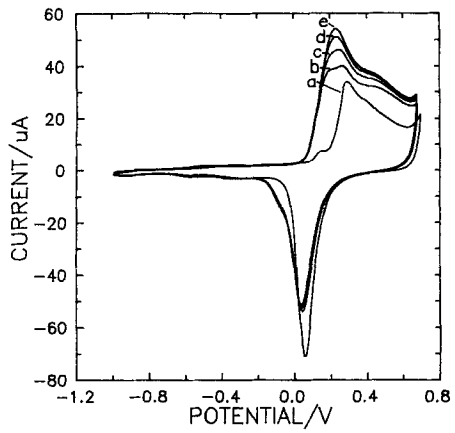

Fig. 4. Voltammetric results for ethylamine at the Au RDE as a function of rotational velocity. Ethylamine concentration (μM): a) 0, b)–e) 40 μM. Scan rate: 100 mV s^{-1}. Rotational velocity [rad s^{-1}]: a, b) 10.5; c) 41.9; d) 94.2; e) 168.

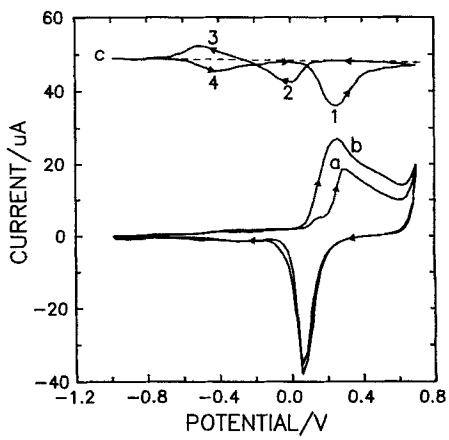

Fig. 5. Voltammetric results for 40 μM ethylamine at Au in 0.1 M NaOH, with PED at the ring electrode. Rotational velocity: 94.2 rad s^{-1}. Disk scan rate: 50 mV s^{-1}. PED waveform at ring: E_{DET} = 0.20 V (t_{DET} = 350 ms, t_{DEL} = 300 ms, t_{INT} = 50 ms; E_{OXD} = 0.80 V (t_{OXD} = 60 ms); E_{RED} = −0.8 V (t_{RED} = 90 ms). Curves: a) disk, residual; b) disk, 40 μM ethylamine; c) ring (10×) 40 μM ethylamine.

Region 2 in curve **c** occurs simultaneously with oxide reduction at the disk electrode as E_d is scanned negative. Because there is little evidence for a corresponding oxidation of ethylamine at the disk in this region (see Fig. 5, curve **b**), we conclude the decreased ring current in Region 2 is the result of adsorption of ethylamine on the oxide-free disk surface. Region 3 in curve **c** (negative scan) corresponds to a ring current in excess of the steady-state value. Because there is no evidence for a simultaneous faradaic reaction at the disk electrode, the peak current in Region 3 is concluded to be the result of desorption of adsorbed ethylamine from the disk surface. The decreased ring current in Region 4 (positive scan) is concluded to be the result of readsorption of ethylamine at the disk surface. These desorption and adsorption phenomena for ethylamine are observed to occur at $E_d = ca.\ -0.5\,V$, which corresponds to the PZC for Au electrodes at pH 13. As discussed above, the small increase in anodic current in the residual response of the disk electrode, obtained during the positive scan for $E_d > -0.5\,V$, has been attributed to the adsorption of OH^-. The correspondence of adsorption processes for OH^- and ethylamine during the positive scan of E_d is evidence of a significant interaction between these species at the Au surface. Further evidence for coadsorption is the observation that desorption of adsorbed ethylamine from the disk surface during the negative scan of E_d occurs concomitantly with cathodic desorption of OH^-.

The absolute values of peak areas in curve **c** of Figure 5 corresponding to desorption (region 3) and readsorption (region 4) are identical. This indicates equivalency for the quantities of ethylamine involved in these two processes. However, the absolute values of the areas under the peak corresponding to adsorption of ethylamine in region 2 is significantly larger than that for desorption of ethylamine in region 3. Hence, we conclude that at least two mechanisms exist for ethylamine adsorption: one involving direct chemisorption to oxide-free Au atoms and the second involving coadsorption with OH^-. More specifically, based on a comparison of the peak areas in Regions 2 and 3, reversible coadsorption of ethylamine with OH^- is concluded to represent ca. 75% of the total quantity of ethylamine adsorbed at Au electrodes in 0.10 M NaOH containing 40 μM ethylamine. The other 25% of ethylamine adsorption appears irreversible and thus is concluded to involve chemisorption of ethylamine to the Au surface.

Further quantitative interpretation of RRDE data is based on the assumption that the total anodic signal for oxidation of ethylamine at the disk electrode ($i_{d,tot}$) in the region *ca.* $0.0 \le E_d \le 0.7\,V$ (postive scan) is the sum of contributions from three sources: (i) current for the formation of surface oxide (designated $i_{d,oxid}$) as is approximated by the residual response in the absence of ethylamine (Fig. 2); (ii) current from oxidative desorption of ethylamine (designated $i_{d,ads}$) that has been preadsorbed on the reduced surface at $E_d < 0.0$ V; and (iii) current from oxidation of ethylamine transported to the disk surface simultaneously with the oxidation process (designated $i_{d,trans}$) at $E_d > 0.0\,V$. Curve **a** in Figure 6 is a plot of total current for ethylamine oxidation ($i_{d,ads} + i_{d,trans}$) as a function of E_d (pos. scan) calculated as the difference between curves **a** and **b** in Figure 5, i.e., $i_{d,tot} - i_{d,oxid}$. The contribution from $i_{d,trans}$ can be calculated from the decrease in ring current below the steady-state value shown in region 1 of Figure 5. This decrease is designated Δi_r. The corresponding value of $i_{d,trans}$ is calculated by dividing Δi_r by the collection efficiency (0.220) for this RRDE and is represented by curve **b** in Figure 6. It is significant that $i_{d,trans}$ accounts

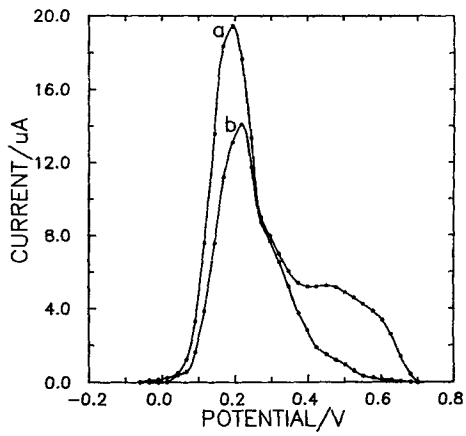

Fig. 6. Disk current vs. disk potential for 40 μM ethylamine with residual current subtracted. Rotational velocity: 94.2 rad s^{-1}. Disk scan rate: 50 mV s^{-1}. Curves: a) total disk current for ethylamine; b) portion of disk current attributable to ethylamine transported to the electrode surface concurrently with the oxidation process ($i_{d,trans}$).

for nearly 100% of $i_{d,tot}$ in the region $0.25\,V \le E_d \le 0.35\,V$. However, for $E_d > 0.4$ V, virtually none of the total disk signal is from ethylamine transported to the disk surface; instead it is from the oxidative desorption of preadsorbed ethylamine.

The potential-dependent nature of the disk response is illustrated also by curves in Figure 7. Curve **a** corresponds to the normalized total disk signal from the oxidation of ethylamine integrated with respect to E_d, i.e., $\int(i_{d,trans} + i_{d,ads})\partial E_d$, during the positive scan for 40 μM ethylamine. By definition, the limiting value in curve **a** reaches unity at the positive scan limit of 0.70 V. Curve **b** represents the contribution from transported ethylamine, i.e., $\int i_{d,trans}\partial E_d$, and curve **c** represents the contribution from preadsorbed ethylamine, i.e., $\int i_{d,ads}\partial E_d$. These data indicate for $0.1\,V \le E_d \le 0.40\,V$ that oxidation of pre-adsorbed ethylamine contributes relatively little to the total response. In contrast, for $E_d >$ ca. 0.4 V, the major contributor to ethylamine signal is the oxidative desorption of preadsorbed ethylamine.

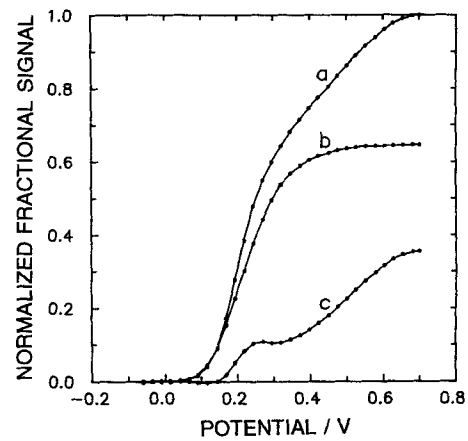

Fig. 7. Normalized integrated disk signal for 40 μM ethylamine as a function of disk potential. Rotational velocity: 94.2 rad s^{-1}. Disk scan rate: 50 mV s^{-1}. Curves: a) total disk signal from ethylamine, b) disk signal due to ethylamine transported to the electrode concurrently with the oxidation process, c) disk signal due to oxidation of preadsorbed ethylamine.

3.4. Determination of *n* for Oxidation of Ethylamine

Values of n (eq mol^{-1}) for transport-limited reactions at rotated disk electrodes can be estimated using the linear relationship between i_d and $\omega^{-1/2}$ as predicted by Equation 1. However, values of i_d for ethylamine oxidation at 0.2 V (positive scan) exhibit a linear dependence on $\omega^{1/2}$ over a very limited range of ω values. The region of linear correspondence was extended somewhat by application of the PED waveform to the rotated disk electrode. The plot of PED response for 5.0 μM ethylamine was observed to be a linear function of $\omega^{1/2}$ over the approximate range $\omega = 12$ to 100 rad s^{-1}. Using the values $u = 0.0104$ cm^2 s^{-1} for 0.10 M NaOH [35] and $D = 1.3 \times 10^{-5}$ cm^2 s^{-1} for ethylamine [36], the value of n was estimated to be 4.0 eq mol^{-1}, with a standard deviation of 0.3 eq mol^{-1}, on the basis of the slopes from i_d-$\omega^{-1/2}$ plots obtained in four trials using 5.0 μM ethylamine. Values for n were found to decrease for increasing ethylamine concentrations. Whereas the reason for the decrease in the calculated n is not known at this time, fouling of the electrode surface is suspected at the higher concentrations.

Previous work at various metal and metal oxide electrodes [6,12,37] has concluded that the product of ethylamine oxidation in aqueous media can be either acetaldehyde (2 eq mol^{-1}) or acetonitrile (4 eq mol^{-1}). Voltammetric studies of acetaldehyde at the Au disk electrode in 0.10 M NaOH (data not shown) indicate this compound is readily oxidized to produce a transport-limited anodic current in the region −0.50 to 0.10 V. Furthermore, acetaldehyde can be detected at the ring of the RRDE under conditions of constant potential. Nevertheless, ring-disk experiments using a constant ring potential (−0.2 V) detected no ring current corresponding to any product of ethylamine oxidation at the disk electrode. Therefore, we conclude that the oxidation product for 5.0 μM ethylamine in 0.1 M NaOH is acetonitrile.

3.5. Estimation of Surface Coverage by Adsorbed Ethylamine

Ring-disk data can be used to estimate both the surface coverages by coadsorbed and chemisorbed ethylamine at the Au disk. For example, in 40 μM ethylamine the ring current indicates that approximately 35% of the total disk current is the result of oxidative desorption of pre-adsorbed ethylamine. Multiplying the total current generated for ethylamine at the disk by 0.35 yields the fraction of disk signal due to preadsorbed ethylamine. Once the current from preadsorbed ethylamine is integrated to yield charge (Q), it can be converted into moles of ethylamine using:

$$N = Q/nF \qquad (2)$$

where N is number of moles and n is assumed to be 4 eq mol^{-1}. Multiplication of N by Avogadro's number (6.0×10^{23}) gives the number of molecules of preadsorbed ethylamine. For this illustration of the applicability of a RRDE to the study of amine adsorption, the true area of the Au electrode is assumed equal to the geometric area ($A_{true} = A_{geo}$), i.e., a surface roughness of unity [38], and a density of Au sites estimated to be 1.3×10^{15} atoms cm^{-2}. Based on ring-disk data, the fractional coverage by adsorbed ethylamine is estimated to be constant at the value 0.7, with a standard deviation of 0.1, over a concentration range of 10 to 60 μM ethylamine, *i.e.*, $1.5 \pm 0.2 \times 10^{-9}$ mol cm^{-2}. Of this amount, approximately 75% is reversibly coassorbed with OH$^-$ and 25% is irreversibly adsorbed by a process concluded to be chemisorption.

4. Conclusions

Data presented here illustrate the applicability of a Au–Au RRDE to a study of the complex voltammetric behavior of ethylamine, as an example of aliphatic amines, on Au electrodes in alkaline media. This demonstration was made possible by the use of a pulsed waveform at the ring electrode to achieve detection of this compound that does not give a persistent signal under conditions of a constant applied potential. The data obtained have demonstrated that oxidation of ethylamine occurs concomitantly with formation of surface oxide. Therefore, the anodic reaction is concluded to occur by an electrocatalytic mechanism coupled with formation of the oxide. The total anodic current for ethylamine oxidation is concluded to originate from oxidative desorption of ethylamine preadsorbed at the reduced disk surface and oxidation of ethylamine transported to the disk surface simultaneously with oxide formation. Ring-disk data indicate ethylamine adsorption occurs via at least two mechanisms: irreversible chemisorption directly on reduced Au sites and reversible coadsorption with OH$^-$. The surface coverage for total adsorbed ethylamine was estimated to be less than one monolayer. Furthermore, it is estimated that approximately 75% of the total adsorbed ethylamine is reversibly co-adsorbed with OH$^-$.

Ring-disk data also permitted quantitative estimations of the contributions to total disk current from each of the processes occurring simultaneously. At the potential of maximum anodic current (ca. 0.2 V, positive scan), corresponding to the onset of oxide formation, oxidation of preadsorbed ethylamine constitutes approximately 35% of the total current for 40 μM ethylamine. However, at potentials > 0.4 V, oxidation of preadsorbed ethylamine constitutes nearly 100% of the ethylamine current.

The product of ethylamine oxidation at Au electrodes in 0.10 NaOH is concluded to be acetonitrile. This conclusion explains some of the differences between the response for ethylamine and ethanolamine at Au electrodes in alkaline media. Oxidation of ethanolamine results in the conversion of the alcohol functional group to the carboxylate anion. The product, a glycinate anion, is very hydrophilic and is believed to be quickly desorbed from the Au surface which allows the surface sites to be recycled within the electrocatalytic mechanisms. As a result, the anodic current for ethanolamine at Au in 0.10 M NaOH is transport limited over a large potential region at the oxide-free electrode surface. Conversely, the likely product of ethylamine oxidation, acetonitrile, has been well-documented to be strongly adsorbed to metal electrodes. Therefore, we speculate that formation of acetonitrile ultimately poisons the Au surface for oxidation of ethylamine and, thus, necessitates potential excursions into potential regions for oxide formation and reduction to bring about desorption of acetonitrile and the subsequent reactivation of the electrode surface.

5. Acknowledgement

This work was supported by the National Science Foundation under Grants CHE-14700 and CHE-9215963.

6. References

[1] K. Stulík, V. Pacáková, K. Le, B. Hennissen, *Talanta* **1988**, *35*, 455.
[2] J.S. Banait, G. Singh, P.K. Pahil, *J. Electrochem. Soc. India* **1984**, *33*, 173.

[3] N.A. Hampson, J.B. Lee, K.I. MacDonald, *J. Electroanal. Chem.* **1972**, *34*, 91.
[4] G. Horanyi, E.M. Rizmayer, *J. Electroanal. Chem.* **1986**, *198*, 393.
[5] C.K. Mann, *Anal. Chem.* **1964**, *36*, 2424.
[6] K.K. Barnes, C.K. Mann, *J. Org. Chem.* **1967**, *32*, 1474.
[7] V.A. Bogdanovskaya, A. Yu. Safronov, M.R. Tarasevich, A.S. Chernyak, *J. Electroanal. Chem.* **1986**, *202*, 147.
[8] B. Malfoy, J.A. Reynaud, *J. Electroanal. Chem.* **1980**, *114*, 213.
[9] A. Yu. Safronov, M.R. Tarasevich, V.A. Bogdanovskaya, A.S. Chernyak, *Elektrokhim.* **1983**, *19*, 421.
[10] N.A. Hampson, J.B. Lee, K.I. MacDonald, *Electrochim. Acta* **1972**, *17*, 921.
[11] N.A. Hampson, J.B. Lee, J.R. Morley, K.I. MacDonald, B. Scanlon, *Tetrahedron* **1970**, *26*, 1109.
[12] N.A. Hampson, J.B. Lee, J.R. Morley, B. Scanlon, *Can. J. Chem.* **1969**, *47*, 3729.
[13] M. Fleishmann, K. Korinek, D. Pletcher, *J. Chem. Soc. Perkin Trans. II* **1972**, *10*, 1396.
[14] P. Cox, D. Pletcher, *J. Appl. Electrochem.* **1991**, *21*, 11.
[15] D. Pletcher, M. Fleishmann, K. Korinek, *J. Electroanal Chem.* **1971**, *33*, 478.
[16] A. Mohammad, I. Haque, *Pak. J. Sci. Res.* **1977**, *29*, 50.
[17] D.C. Johnson, D. Dobberpuhl, R. Roberts,, P. Vandeberg, *J. Chromatogr.* **1993**, *640*, 79.
[18] W.A. Jackson, W.R. LaCourse, D.A. Dobberpuhl, D.C. Johnson, *Electroanalysis* **1991**, *3*, 607.
[19] D.A. Dobberpuhl, D.C. Johnson, *Anal. Chem.* **1995**, *34*, 1254.
[20] V.G. Levich, *Physicochemical Hydrodynamics*, Prentice-Hall, Englewood Cliffs, N J, **1962**, pp. 60–72.
[21] D.W. Kirk, F.R. Foulkes, W.F. Graydon, *J. Electrochem. Soc.* **1980**, *127*, 1069.
[22] G.N. Van Huong, C. Hinnen, J. Lecoeur, *J. Electroanal. Chem.* **1980**, *107*, 185.
[23] L.D. Burke, M.E. Lyons, D.P. Whelan, *J. Electroanal. Chem.* **1982**, *139*, 131.
[24] S. Bruckenstein, M. Shay, *J. Electroanal. Chem.* **1985**, *188*, 131.
[25] J. Desilvestro, M.J. Weaver, *J. Electroanal. Chem.* **1986**, *209*, 377.
[26] H. Angerstein-Kozlowska, B.E. Conway, *Electrochim. Acta* **1986**, *31*, 1051.
[27] G.N. Van Huong, C. Hinnen, J. Lecoeur, R. Parsons, *J. Electroanal. Chem.* **1978**, *92*, 239.
[28] C. Hinnen, G.N. Van Huong, A. Rousseau, J.P. Dalbera, *J. Electroanal. Chem.* **1980**, *106*, 175.
[29] J.S. Gordon, D.C. Johnson, *J. Electroanal. Chem.* **1994**, *365*, 267.
[30] L.D. Burke, V.J. Cunnane, *J. Electroanal. Chem.* **1986**, *210*, 69.
[31] J.E. Vitt, L.A. Larew, D.C. Johnson, *Electroanalysis* **1990**, *2*, 21.
[32] L.D. Burke, K.J. O'Dwyer, *Electrochim. Acta* **1990**, *35*, 1829.
[33] L.D. Burke, B.H. Lee, *J. Electroanal. Chem.* **1992**, *330*, 637.
[34] L.D. Burke, J.F. O'Sullivan, *Electrochim. Acta* **1992**, *37*, 585.
[35] *CRC Handbook of Chemistry, Physics*, 59th ed. (Ed: R.C. Weast) CRC Press, Boca Raton, FL, **1979**, p. D-303.
[36] A.N. Cambell, S.Y. Lam, *Can. J. Chem.* **1973**, *51*, 4005.
[37] R.C. Reed, R.M. Wightman, in *Encyclopedia of Electrochemistry of the Elements* Vol. XV, (Eds: A.J. Bard, H. Lund), Marcel Dekker, New York **1984**, pp. 1–165.
[38] J.F. Rodriguez, T. Mebrahtu, M.P. Soriaga, *J. Electroanal. Chem.* **1987**, *233*, 283.